Supplemental material

Sandrock et al., https://doi.org/10.1084/jem.20181439

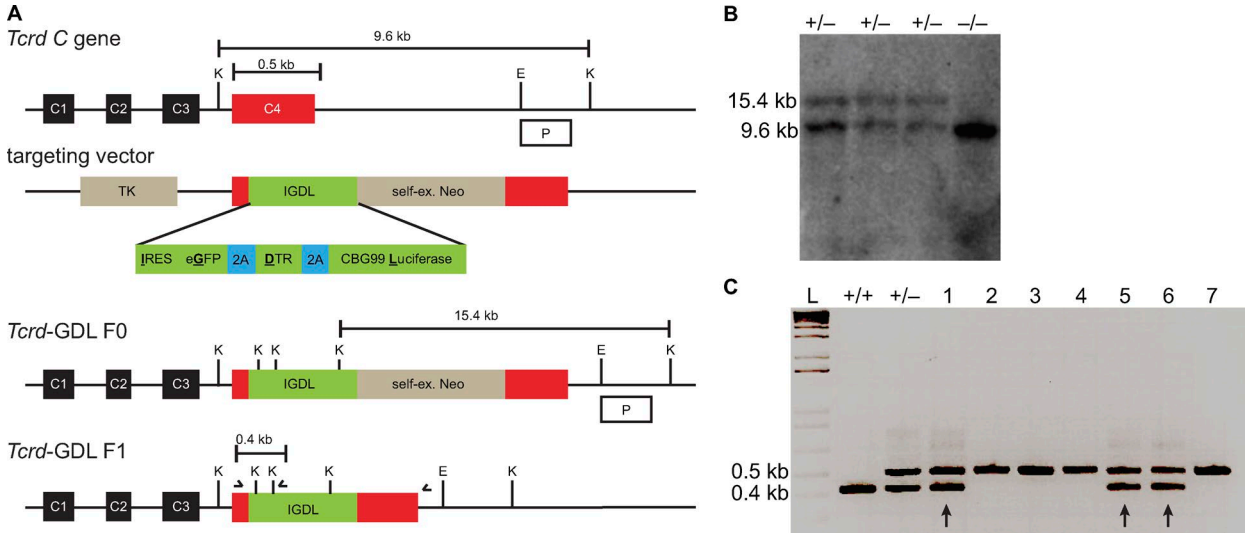

Figure S1. **Generation of the *Tcrd*-GDL mouse line. (A)** Strategy used to generate *Tcrd*-GDL mice. The *Tcrd* constant (*Tcrd* C) gene in JM8A3 mouse embryonic stem cells was targeted with a vector containing an expression cassette encoding for eGFP, human DTR, and green click beetle luciferase (CBG88 luciferase) separated by 2A self-cleaving sites (kindly provided by Prof. Hämmerling, German Cancer Research Center, Heidelberg, Germany). C1–C4: exons of the *Tcrd* C gene; E: EcoRI restriction site; K: KpnI restriction site; P: probe used for Southern blot; self-ex. Neo: self-excising neomycin resistance cassette after germline transmission; TK: tyrosine kinase. F0: founder mice; F1: F1 generation (angles indicate primers used for genotyping). **(B)** Southern blot to detect integration of the expression cassette into the *Tcrd* C gene. +/–: clones that were tested positive for integration by PCR; –/–: clone that was tested negative for integration by PCR. **(C)** Germline transmission was tested in F1 mice by PCR. WT: 0.5 kp; GDL: 0.4 kb. Offspring (1–7) positive for the GDL knock-in are indicated by arrows. For +/+ and +/–, control genomic DNA of homozygous and heterozygous *Tcrd*-H2BeGFP mice, respectively, was used as they were generated with a similar strategy.

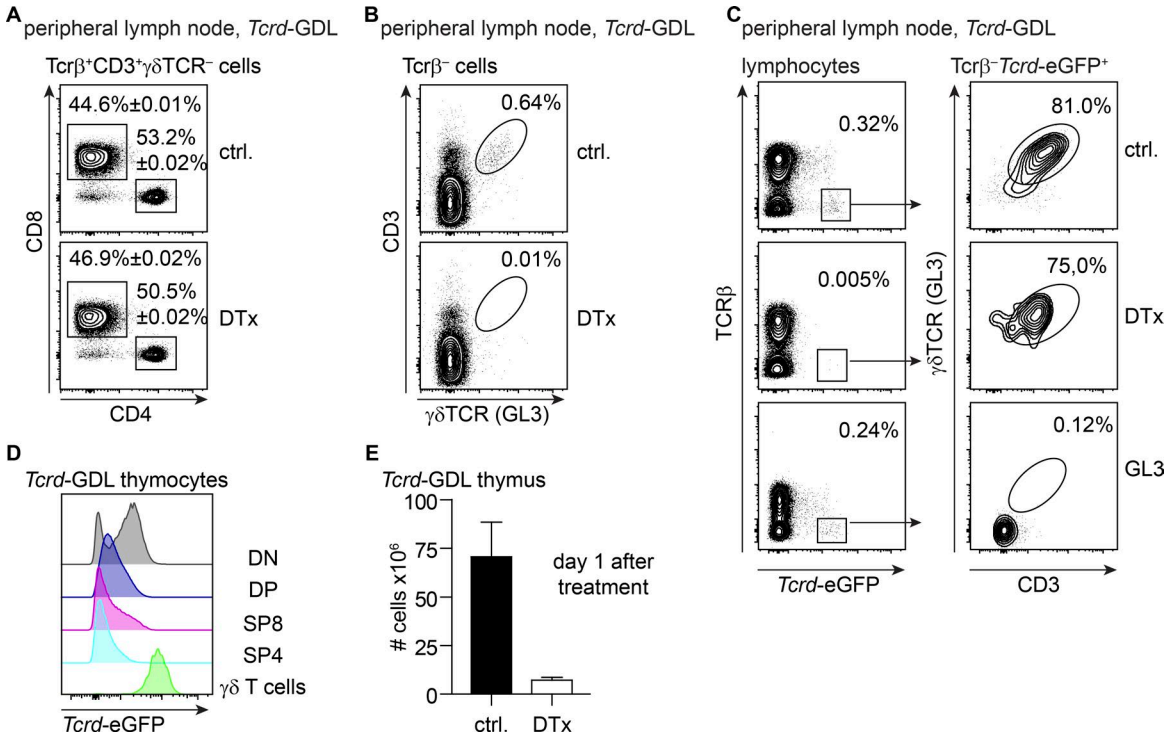

Figure S2. **DTx specifically depletes γδ T cells in *Tcrd*-GDL mice. (A–C)** Contour plots of peripheral lymph node γδ T cells from *Tcrd*-GDL mice treated i.p. with PBS (ctrl.), DTx (day 1 after depletion), or pan-γδTCR antibody (clone GL3; day 1 after injection). Shown are representative data from at least two independent experiments with $n = 1–4$ mice each. **(A)** Composition of CD4 CD8 αβ T cell compartment is not affected by DTx treatment. Frequencies of CD8 and CD4 αβ T cells in nondepleted (ctrl.) and γδ T cells depleted (DTx) mice, respectively. **(B)** DTx efficiently depletes γδ T cell analyzed by staining for CD3 and pan-γδTCR. **(C)** Frequencies of GFP+ γδ T cells and surface staining of CD3 and γδTCR after treatment with DTx or pan-γδTCR antibody (GL3). **(D and E)** Flow cytometric analysis of Tcrd-GDL thymocytes. Data from one representative experiment of at least two with $n = 2$ mice each. **(D)** eGFP fluorescence intensity of indicated cell populations among *Tcrd*-GDL thymocytes. Double-negative (DN) thymocytes were defined as $CD4^-CD8^-\gamma\delta TCR^-$, CD4 single-positive (SP4) thymocytes were defined as $CD4^+CD8^-$, CD8 single-positive (SP8) thymocytes were defined as $CD4^-CD8^+$, and γδ T cells were defined as $CD4^-CD8^-\gamma\delta TCR^+CD3^+$. **(E)** Thymus cellularity in γδ T cell nondepleted control (ctrl.) and DTx-treated *Tcrd*-GDL mice 1 d after depletion.

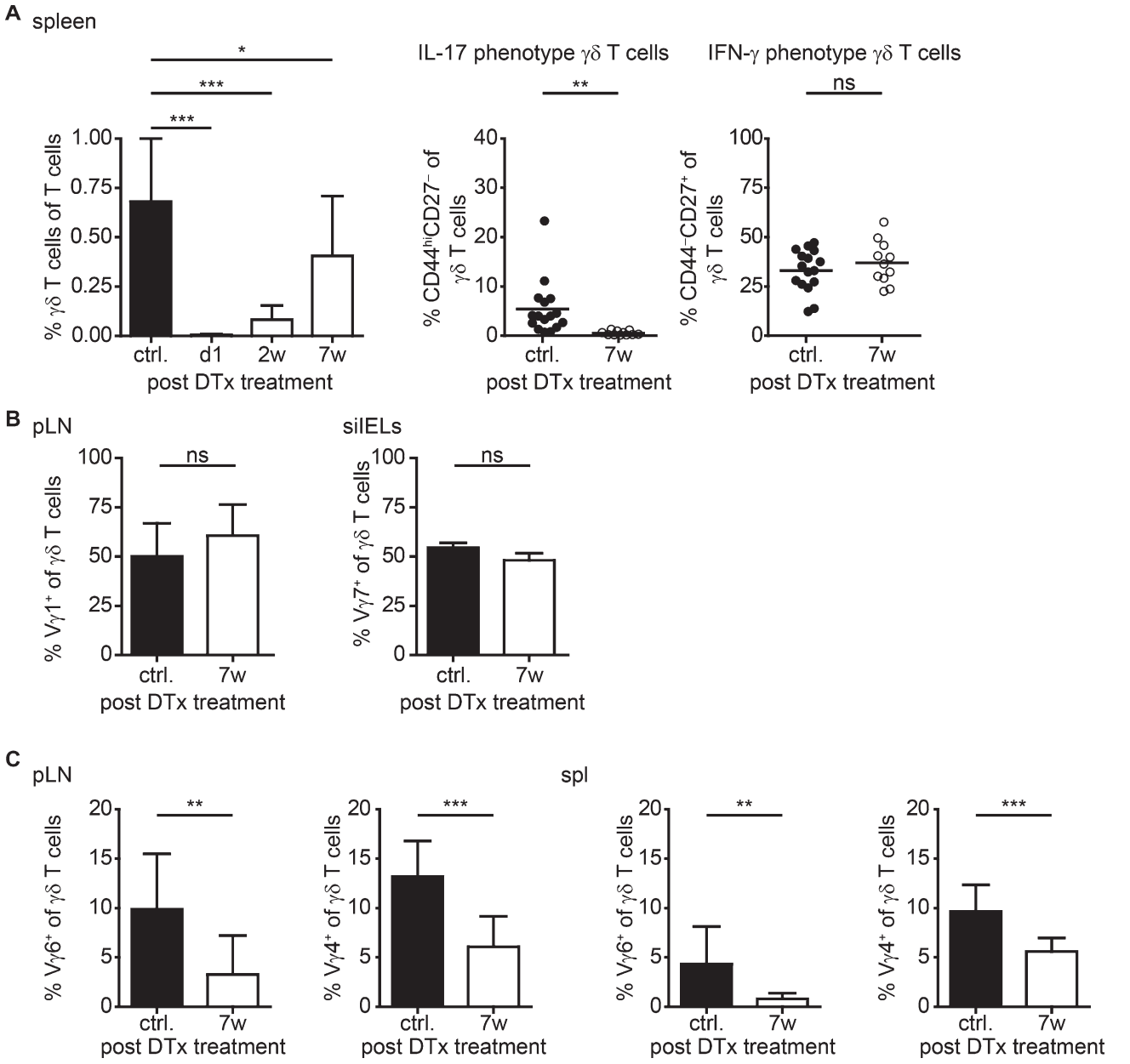

Figure S3. **In secondary lymphoid organs Tγδ17 cells recover inefficiently. (A–C)** Flow cytometric analysis of indicated cell populations 1 d (d1), 2 wk (2w), and 7 wk (7w) after depletion of γδ T cells in *Tcrd*-GDL littermates. **(A)** Frequencies of splenic γδ T cells (Tcrβ$^-$GFP$^+$) among T cells (A.dead$^-$CD3$^+$; left, mean ± SD, ANOVA with Bonferroni posttests), IL-17 phenotype (CD44^{hi}CD27$^-$; middle, mean), and IFN-γ phenotype (CD44$^-$CD27$^+$; right, mean) γδ T cells; one dot equals one mouse, Student's *t* test. Shown are pooled data from three independent experiments with each n = 2–5 mice per group. **(B)** Frequencies of peripheral lymph node Vγ1$^+$ γδ T cells, mean ± SD, Student's *t* test. Shown are pooled data from two independent experiments with each n = 2–4 mice per group (left). Frequencies of Vγ7$^+$ small intestinal intraepithelial lymphocyte (silEL) γδ T cells, mean ± SD, Student's *t* test. Shown are pooled data from n = 2–3 mice per group (right). **(C)** Frequencies of Vγ6$^+$ and Vγ4$^+$ γδ T cells, respectively, in peripheral lymph nodes (left) and spleen (right), mean ± SD, Student's *t* test. Shown are pooled data from three independent experiments with each n = 2–5 mice per group. *, P < 0.05; **, P < 0.01; ***, P < 0.001; ns, not significant.

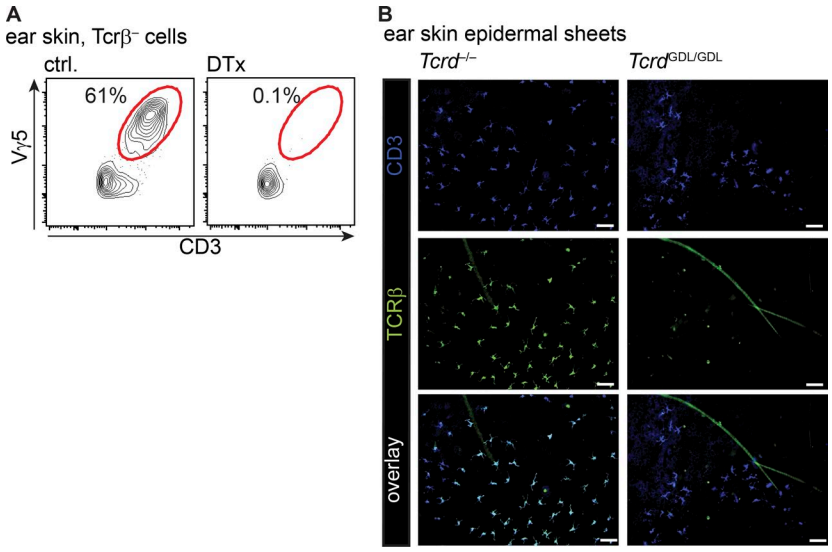

Figure S4. **DTx efficiently depletes DETCs and the niche is not refilled by TCRβ⁺ cells. (A)** Representative contour plots of ear skin lymphocytes gated on Tcrβ⁻ cells from littermate *Tcrd*-GDL mice treated with PBS (ctrl.) or DTx. **(B)** Representative epidermal sheet fluorescence microscopy images of γδ T cell depleted *Tcrd*-GDL mice 5 wk after depletion compared with *Tcrd*$^{-/-}$ mice. Blue: CD3; green: TCRβ. Bars, 50 µm. **(A and B)** Data are representative of at least two experiments.

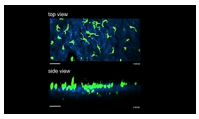

Video 1. **In vivo two-photon imaging of *Tcrd*-GDL ear skin.** Top view (upper) and side view (lower) of steady state ear skin. Green: γδ T cells, *Tcrd*-GDL GFP; blue: collagen, second harmonics signal. Bars, 50 µm. Time in h:min:sec.

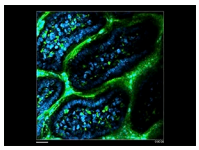

Video 2. **In vivo two-photon imaging of *Tcrd*-GDL small intestine.** A section of the small intestine was externalized and opened longitudinally at the anti-mesenteric side for imaging. Imaging was performed with the luminal side up. Green: γδ T cells, *Tcrd*-GDL GFP; blue: nuclei, Hoechst 33342. Bar, 30 µm. Time in h:min:sec.

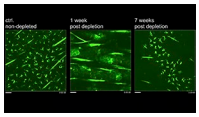

Video 3. **Longitudinal in vivo two-photon imaging of *Tcrd*-GDL ear skin after depletion of γδ T cells.** Videos were acquired from the same mouse at indicated time points after γδ T cell depletion. As reference, a mouse was injected with PBS (ctrl.). Green: γδ T cell eGFP by *Tcrd*-GDL mice. Shown are representative videos of two independent experiments. Bars, 50 µm. Time in h:min:sec.

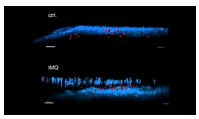

Video 4. **In vivo two-photon imaging of inflamed and healthy ear skin.** Videos were acquired from healthy, noninflamed (ctrl.) and inflamed psoriatic (IMQ) ear skin; ears were treated for four to seven consecutive days. Shown are representative videos of three experiments with each one to two mice per group, *Tcrd*-GDL and *Tcrd*-H2BeGFP mice. Red dots: tracked motile dermal γδ T cells blue: collagen, second harmonics signal. Time in h:min:sec.